

RESEARCH

Open Access



# Comparative transcriptome analysis reveals the impact of daily temperature difference on male sterility in photo-thermo-sensitive male sterile wheat

Fuqiang Niu<sup>1†</sup>, Zihan Liu<sup>2†</sup>, Yongjie Liu<sup>2†</sup>, Jianfang Bai<sup>2</sup>, Tianbao Zhang<sup>2</sup>, Shaohua Yuan<sup>2</sup>, Xiucheng Bai<sup>2</sup>, Changping Zhao<sup>2</sup>, Fengting Zhang<sup>2</sup>, Hui Sun<sup>2\*</sup>, Liping Zhang<sup>2\*</sup>, Liping Zhang<sup>2\*</sup> and Xiyue Song<sup>1\*</sup>

## Abstract

**Background** Photo-thermo-sensitive male sterility (PTMS), which refers to the male sterility triggered by variations in photoperiod and temperature, is a crucial element in the wheat two-line hybrid system. The development of safe production and efficient propagation for male sterile lines holds utmost importance in two-line hybrid wheat. Under the stable photoperiod condition, PTMS is mainly induced by high or low temperatures in wheat, but the effect of daily temperature difference (DTD) on the fertility conversion of PTMS lines has not been reported. Here, three BS type PTMS lines including BS108, BS138, and BS366, as well as a control wheat variety J411 were used to analyze the correlation between fertility and DTD using differentially sowing tests, photo-thermo-control experiments, and transcriptome sequencing.

**Results** The differentially sowing tests suggested that the optimal sowing time for safe seed production of the three PTMS lines was from October 5th to 25th in Dengzhou, China. Under the condition of 12 h 12 °C, the PTMS lines were greatly affected by DTD and exhibited complete male sterility at a temperature difference of 15 °C. Furthermore, under different temperature difference conditions, a total of 20,677 differentially expressed genes (DEGs) were obtained using RNA sequencing. Moreover, through weighted gene co-expression network analysis (WGCNA) and KEGG enrichment analysis, the identified DEGs had a close association with “starch and sucrose metabolism”, “phenylpropanoid biosynthesis”, “MAPK signaling pathway-plant”, “flavonoid biosynthesis”, and “cutin, and suberine and wax biosynthesis”. qRT-PCR analysis showed the expression levels of core genes related to KEGG pathways significantly

<sup>†</sup>Fuqiang Niu, Zihan Liu and Yongjie Liu contributed equally to this work.

\*Correspondence:

Hui Sun  
Sunhui628@sina.com  
Liping Zhang  
lpzhang8@126.com  
Xiyue Song  
songxiyue@nwafu.edu.cn

Full list of author information is available at the end of the article



decreased at a temperature difference of 15 °C. Finally, we constructed a transcriptome mediated network of temperature difference affecting male sterility.

**Conclusions** The findings provide important theoretical insights into the correlation between temperature difference and male sterility, providing guidance for the identification and selection of more secure and effective PTMS lines.

**Keywords** Daily temperature difference, Male sterility, Safe seed production, Transcriptome, Wheat

## Background

Given the growing population and shrinking arable land, it has become crucial to rely on technological advancements to enhance the yield per unit area as a solution to the food problem [1]. One of the most effective approaches is harnessing heterosis to increase grain crop yield [2]. The utilization of heterosis in wheat (*Triticum aestivum* L.) has been extensively studied both domestically and internationally, and is considered an important approach to significantly increase wheat yield in the future. However, the widespread use of hybrid wheat in production is severely limited due to challenges such as the large amount of seed required, low yield of hybrid seed production, high production costs, and the difficulty in seed production [3]. Therefore, the research and development of safe, high-yield, stable-yield, and cost-effective seed production techniques are crucial for promoting the widespread adoption of hybrid wheat.

Male sterility, a phenomenon of male organ loss of physiological function, can be attributed to several factors, such as abnormal anther morphology, decreased pollen vitality, abnormal pollen structure, and nutrient deficiency. Abnormal development of anther morphology, such as thin and small anthers, as well as indehiscent anthers, can ultimately result in male sterility [4, 5]. Pollen, as an important carrier of genetic information transmission, is an indispensable material for plant genetic breeding, hybrid seed production, and germplasm preservation. The decrease in pollen vitality can affect the fertilization process, leading to a decrease in seed setting rate [6, 7]. Furthermore, the formation of the pollen wall is crucial for the proper growth and development of pollen grains, making it one of the pivotal structures. The aberrations in the intine and exine development further contribute significantly to male sterility [5, 8]. Moreover, during the growth and development process, anthers require a significant amount of nutrients to accumulate, and any abnormal fluctuations in the levels of these substances can lead to alterations in fertility. Studies have shown that the shortage of soluble sugars, starch, soluble proteins, and free proline content inhibits anther development, resulting in the manifestation of male sterility [9–11]. However, it is not yet known whether the daily temperature difference (temperature fluctuation) affects plant male fertility.

Male sterility can be categorized into two types: environmentally sensitive male sterility known as photo-thermo-sensitive male sterility (PTMS), and non-environmentally sensitive male sterility, which can be further classified as genic male sterility or cytoplasmic male sterility. In PTMS line, the development of male gametes and expression of fertility are regulated by variations in light and temperature during spike differentiation and development [12]. The majority of PTMS are characterized by male sterility at low temperature short-day conditions, while manifested as male fertility at long-day high temperature conditions in wheat. And the PTMS line has the characteristics of wide recovery sources, simplified hybrid seed production procedures, and good commercialization, and has become one of the main ways to utilize wheat heterosis. In recent years, several types of wheat PTMS lines have been discovered and utilized, such as the C49S line [13], ES line [14], BS type [15], LT-1–3 A type [16], BNS type [17], and 337 S type [18]. The BS type PTMS lines (BS20 and BS210) was induced by short-day and low temperature during the connectivum formation to the uninucleate stage. The critical temperature for BS20 and BS210 was 10~12 °C and 8~12 °C [12, 19]. C49S was sensitive to light and temperature during meiosis and microsporogenesis stage, with a critical temperature range of 12~14 °C and a critical light duration of 12 h [20]. ES-10 was induced by light and temperature from the pistil and stamen differentiation to the tetrad formation period. The critical light duration for ES-10 was less than 11.5 h, and the critical temperature range was 9~11 °C [21]. The sensitive period for BNS extended from pistil and stamen differentiation period to the tetrad formation period, with a critical temperature range of 8~12 °C [22]. 337 S was sterile under short-day low temperature and long-day high temperature conditions during the panicle differentiation stage, but it became fertile when sowed at the appropriate date [23]. To date, several studies have been conducted to examine the fertility conversion of PTMS lines in wheat, however, the influence of different DTDs on the conversion of fertility in male sterile lines remains unreported within the context of consistent average temperature.

The wheat BS type PTMS lines offer several advantages, including stable fertility, excellent seed production traits, and good general combining ability [24, 25]. As a result,

numerous hybrid wheat varieties have been approved using the sterile lines. In this study, the influence of DTD on the fertility of sterile lines was examined by combining staged sowing identification and photo-thermo-control experiments using wheat BS type PTMS lines (BS108, BS138, and BS366) and conventional wheat J411 as materials. Transcriptome analysis was conducted to identify DEGs and key metabolic pathways associated with DTD. Additionally, the identification of pivotal genes associated with DTD was carried out by WGCNA. These findings significantly enhance the theoretical comprehension of the mechanism behind fertility conversion in male sterile lines that respond to photo-thermal changes. Additionally, it greatly supports the attainment of large-scale, secure, and productive seed manufacturing.

## Materials and methods

### Plant materials

BS (Beijing Sterile) type photo-thermo-sensitive genic male sterility lines, BS108, BS138, and BS366, were employed as research materials, along with the conventional wheat J411 in this study. The formal identification of the BS type PTMS lines BS108, BS138, and BS366 were undertaken by Professor Hui Sun and Fengting Zhang (Institute of Hybrid Wheat, Beijing Academy of Agriculture and Forestry Sciences, Beijing, China). And the formal identification of the conventional wheat J411 were undertaken by Professor Zhangming Li (Beijing Seed Company, Beijing, China). The BS type PTMS lines BS108, BS138, and BS366 were preserved at the Crop Germplasm Resource Genebank of Beijing with voucher numbers YZ002714, YZ002733, and YZ003399, respectively. And the conventional wheat J411 was conserved at the National Germplasm Resource Genebank of China with voucher numbers ZM020984. The wheat PTMS line BS366 originated from a natural mutant of doubled haploid lines resulting from the cross of Jingdong8121/E8075-7. BS108 was selected from the offspring of the hybrid combination BS366/Luomai 1. And BS138 is an improved line of the wheat PTMS line BS210, which is derived from single plants selected from the common wheat combination (Beinong 2/Jimai 36). These BS type PTMS lines were screened and cultivated by the Beijing Academy of Agriculture and Forestry and displayed a sterility phenotype in low temperature short-day conditions (Dengzhou, Henan; 34°40'N, 112°21'E), but exhibits fertility in long-day high temperature conditions (Shunyi, Beijing; 40°08'N, 116°39'E). An examination of anthers from BS108, BS138, BS366, and J411 under different temperature differences was performed using RNA-Seq analysis. To ensure the preservation of RNA integrity, the collected samples underwent immediate freezing in liquid nitrogen and were later stored at -80 °C. Each of the

collected samples was independently replicated in three biological replicates.

### Differentially sowing test

In order to determine the optimal sowing date for safe seed production in PTMS lines, a sowing date test was conducted in Dengzhou, China (34°40' N, 112°21' E) using the BS108, BS138, BS366, and J411 in the years 2018–2019 and 2019–2020. The sowing periods were set as 5, 10, 15, 20, 25, 30 October, and 4 November, respectively. Moreover, the sowing date with a seed setting rate lower than 2.5% can be defined as a safe sowing date for seed production. Each material, approximately 30 seeds, was planted in rows with a length of 1.50 m, plant spacing of 0.03 m and row spacing of 0.25 m. All tests were managed according to standard procedures.

### Photo-thermo-control experiments

The photo-thermo-control experiments were carried out in a controlled environment chamber. During the experiment, the humidity level was maintained at 70%, ensuring a stable moisture content in the environment. Additionally, the light intensity was maintained at a level of 125  $\mu\text{Mol}/(\text{m}^2 \cdot \text{s})$ , ensuring consistent and sufficient illumination for the study. The experimental seedlings were sown on 1 October in flower pots measuring 26 cm  $\times$  23 cm each. In each pot, there were a total of 8 seedlings. To provide the necessary nutrients, diamine phosphate (0.88 g) and urea (0.63 g) were applied as a base fertilizer. Moreover, at the stage when the seedlings had developed four leaves, an additional topdressing of 0.63 g of urea was performed. Subsequent to the completion of vernalization, the flower pots were relocated to a greenhouse until the seedlings reached the required growth period. Subsequently, the seedlings were relocated to a controlled environment chamber where they were subjected to a series of treatments that included different combinations of light and temperature exposure. Each material was processed in six pots, with eight plants per pot and three replicates. To investigate the fertility conversion characteristics of male sterile lines under different DTDs in light temperature conditions of the seed production area (12 h 12 °C), temperature difference experiments were conducted. The treatment duration was 12 h per day (with the inclusion of additional light from 6:00 to 18:00), and the average temperature was maintained at 12 °C. Two different temperature difference settings were applied, namely temperature difference of 0 °C and temperature difference of 15 °C (Table S1). A temperature difference of 0 °C indicates a constant temperature of 12 °C throughout the day, whereas a temperature difference of 15 °C signifies fluctuating temperatures with a minimum of 4.5 °C and a maximum of 19.5 °C throughout the day.

The treatment period (fertility sensitive period) was from connective to uninucleate stage.

### Phenotypic identification

Florets collected from BS108, BS138, BS366, and J411 at the trinucleate stage were meticulously observed using Motic K400 dissecting microscope (Preiser Scientific, Louisville, KY, USA). The I<sub>2</sub>-KI staining technique was employed to assess the fertility of mature flower pollen grains. These grains were then captured using a stereomicroscope ((SZX10, Olympus, Tokyo, Japan). Additionally, for each main stem spike and 1–2 tiller spikes, precautionary measures were taken by bagging them before flowering. Subsequently, the seed setting rates of the PTMS lines were statistically analyzed after wheat grain filling and maturity. The formula utilized to calculate the rate of seed setting was as follows: Seed setting rate = number of grains per spike / number of spikelets / 2 × 100%.

### Transcriptome sequencing

For transcriptome sequencing, the anthers from BS108, BS138, BS366, and J411 under different DTDs at the tetrad stage were employed to construct cDNA libraries, which containing a total of 24 samples with three biological replicates. RNA isolation was carried out using the RNA Extraction Kit (Invitrogen, Nottingham, UK). In order to evaluate the integrity of RNA and detect any possible DNA contamination, we conducted agarose gel electrophoresis with a concentration of 1%. To validate the integrity of the RNA, the Agilent 2100 bioanalyzer was utilized. Additionally, a NanoPhotometer spectrophotometer was employed to assess the purity of the RNA. The cDNA library construction and quality inspection were conducted following the methods described by Liu et al. [26]. After the libraries passed our quality inspection criteria, they were pooled based on their effective concentration and target offline data volume requirements. Subsequently, the paired-end RNA-seq sequencing was conducted using the Illumina HiSeq2500 platform with a read length of 2 × 150 bp at Shanghai Origene Bio-pharm Technology Co., Ltd.

### Identification and functional annotations of DEGs

We have implemented quality control measures for the raw data to ensure its accuracy and reliability. Following this, we performed alignment of the clean reads to the reference genome of wheat ([https://plants.ensembl.org/Triticum\\_aestivum/Info/Index?db=core](https://plants.ensembl.org/Triticum_aestivum/Info/Index?db=core)) using the HISAT2 v2.0.4 tool. To determine the gene expression levels, we utilized HTSeq v0.6.1 to count the number of gene reads, and then the fragments per kilobase million (FPKM) was calculated. In order to identify expression of differential gene, we performed analysis on four

comparisons: BS108-0 vs. BS108-15, BS138-0 vs. BS138-15, BS366-0 vs. BS366-15, and J411-0 vs. J411-15. For this analysis, we employed the DESeq2 R package (version 1.16.1). Firstly, the initial read count was normalized to adjust for sequencing depth. Subsequently, the difference in gene expression between the two groups was evaluated by computing the fold change of expression values with an absolute fold change > 1. Finally, to account for multiple testing, we adopted the widely-used Benjamini and Hochberg correction method, with a threshold of adjusted p-value (Padj) less than 0.05. Furthermore, to gain insights into the functional annotation of the DEGs, we conducted Gene Ontology (GO) enrichment analysis and Kyoto Encyclopedia of Genes and Genomes (KEGG) enrichment analysis. The enrichment analyses were exclusively conducted on the DEGs that possessed an adjusted p-value (Padj) below 0.05. The Goseq R package and KOBAS 2.0 were used for the GO enrichment analysis and KEGG enrichment analysis, respectively [27].

### Weighted gene co-expression network analysis (WGCNA)

WGCNA can identify gene sets with similar expression patterns and analyze the relationship between gene sets and sample phenotypes. The process of WGCNA is primarily divided into: input data, construction of co-expression network, division of modules, correlation analysis between modules and traits, correlation analysis between modules, and identification of hub genes within modules. To conduct the analysis of DEGs and assess their association with DTD, the WGCNA was utilized using the R package. The key objective was to identify gene modules that exhibit strong co-expression patterns in relation to DTD. To construct the module, we calculated pairwise Pearson's correlation coefficients between genes which helped in creating the adjacency matrix. Next, we advanced to constructing the WGCNA network and evaluating the modules by employing an unsigned type topology overlap matrix. Throughout the investigation, we maintained a constant power  $\beta$  value of 10 and a branch merge cut height of 0.25. In order to gauge the relationship between the module and the daily variation in temperature, we partitioned various modules and identified key modules using correlation analysis with phenotypic data. Subsequent functional enrichment analysis of genes within these key modules was conducted.

### Quantitative real-time PCR (qRT-PCR) analysis

Three PTMS lines (BS108, BS138, and BS366) were used to isolate total RNA from the anthers under different DTDs. The RNA extraction was carried out using the Plant RNA Extraction Kit provided by Roche (Germany), whereas the first-strand cDNA synthesis was conducted using the PrimeScript™ RT Reagent from TaKaRa (China). For quantitative real-time PCR (qRT-PCR), the



QuantStudio™ 7 Flex Real-Time PCR System manufactured by Applied Biosystems (USA) was utilized. The primer sequences required for amplifying hub genes were acquired from the Primer-NCBI website (<https://www.ncbi.nlm.nih.gov/tools/primer-blast/>). The mRNA levels of the hub genes were normalized using *TaActin*, a housekeeping gene (GenBank accession: GQ 339766.1). The quantification of the qRT-PCR data was achieved using the  $2^{-\Delta\Delta CT}$  method. And the data were presented as the means  $\pm$  SD of three biological replicates. Statistical significance was determined using a T-test, with  $*P < 0.05$  indicating significance and  $**P < 0.01$  indicating high significance. The primer sequences for hub genes and *TaActin* can be found in Table S2.

### Statistical analysis

The statistical analyses were conducted using GraphPad Prism version 8.0.1 for Windows, a software developed by GraphPad Software (San Diego, CA, USA, [www.graphpad.com](http://www.graphpad.com)). Duncan's multiple range tests were utilized to compare multiple sets statistically. Additionally, the heatmap was generated using the TBtools software [28], while the network model was created using Adobe Illustrator CS5.

## Results

### Sowing test under different sowing date

To determine the appropriate sowing date for safe seed production of PTMS lines, a sowing test was conducted under different sowing date in Dengzhou (seed production area) during the 2018–2019 and 2019–2020 sowing season. According to the results, during the sowing period from October 5th to 25th, the fertility of the

three PTMS lines was low, with a seed setting rate ranging from 0 to 0.98%, which reached a high level of male sterility and allowed for safe seed production. However, the PTMS lines did not meet the requirements for safe seed production when sown on November 4th. In contrast, the fertility of the control variety J411 was normal at different sowing dates, and no noticeable variation in the seed setting rate was observed throughout the sowing period, as the rates ranged between 99.36% and 100.88% (Table 1). The results were consistent with previous studies on the sowing date of BS type PTMS lines [25], which further confirmed that the best sowing time for safe seed production of BS type PTMS lines was from October 5th to 25th.

### The influence of DTD on the fertility of PTMS lines

To investigate the influence of DTD on the fertility conversion of PTMS lines in the seed production area (Dengzhou), we simulated the environment of the seed production area in artificial climate chamber during the fertility sensitive period, with light duration and temperature of 12 h and 12 °C, respectively [25]. The DTD was tested using two treatments: a temperature difference of 0 °C and a temperature difference of 15 °C. At a temperature difference of 0 °C, the results suggested that the seed setting rates of BS108, BS138, and BS366 were recorded as 7.30%, 17.18%, and 15.25%, respectively. However, the seed setting rates of the PTMS lines significantly decreased to 0.19%, 0.00%, and 0.00% when the temperature difference was increased to 15 °C, respectively. The fertility performance of the control variety, J411, remained normal under different temperature differences, with seed setting rates ranging from 84.40 to 85.74% (Fig. 1 and Table S3). These findings suggested that increasing the temperature difference could reduce the seed setting rate of PTMS lines, which was beneficial for ensuring safe seed production.

**Table 1** Seed setting rate (%) of PTMS lines and J411 in Dengzhou, Henan during the 2018–2019 and 2019–2020

Sowing date (month/day)	BS108	BS138	BS366	J411
2018–2019				
10/5	0.00 f	0.00 e	0.00 f	100.02 a
10/10	0.00 f	0.00 e	0.00 f	100.14 a
10/15	0.12 e	0.00 e	0.23 e	100.06 a
10/20	0.66 d	0.18 d	0.45 d	100.04 a
10/25	0.98 c	0.56 c	0.81 c	100.11 a
10/30	2.74 b	2.64 b	2.52 b	100.17 a
11/4	7.89 a	6.26 a	3.93 a	100.32 a
2019–2020				
10/5	0.00 e	0.00 c	0.00 f	99.36 a
10/10	0.03 e	0.00 c	0.00 f	99.54 a
10/15	0.24 d	0.00 c	0.16 e	99.89 a
10/20	0.84 c	0.00 c	0.32 d	99.98 a
10/25	0.88 c	0.00 c	0.41 c	100.44 a
10/30	3.02 b	0.24 b	1.26 b	100.88 a
11/4	8.91 a	4.88 a	3.76 a	100.21 a

Different letters indicate significant differences in the same male sterile line at different sowing dates ( $p < 0.05$ )

### Phenotypic characteristics for PTMS lines under different DTDs

To investigate the fertility differences of PTMS lines under temperature differences of 0 °C and 15 °C, phenotypic identification was performed on the anthers of BS108, BS138, BS366, and J411 during the trinucleate stage. At a temperature difference of 0 °C, PTMS lines showed partial male sterility, with 10%, 19%, and 14% of pollen from BS108, BS138, and BS366 respectively being able to be stained with I<sub>2</sub>-KI (Fig. 2A and Fig. S1). However, at a temperature difference of 15 °C, PTMS lines exhibited complete male sterility, characterized by shrunken and slender anthers. Moreover, their pollen grains were almost unable to be stained by I<sub>2</sub>-KI (Fig. 2B and Fig. S1). Furthermore, at the trinucleate stage, no noticeable distinctions were witnessed in the anthers of

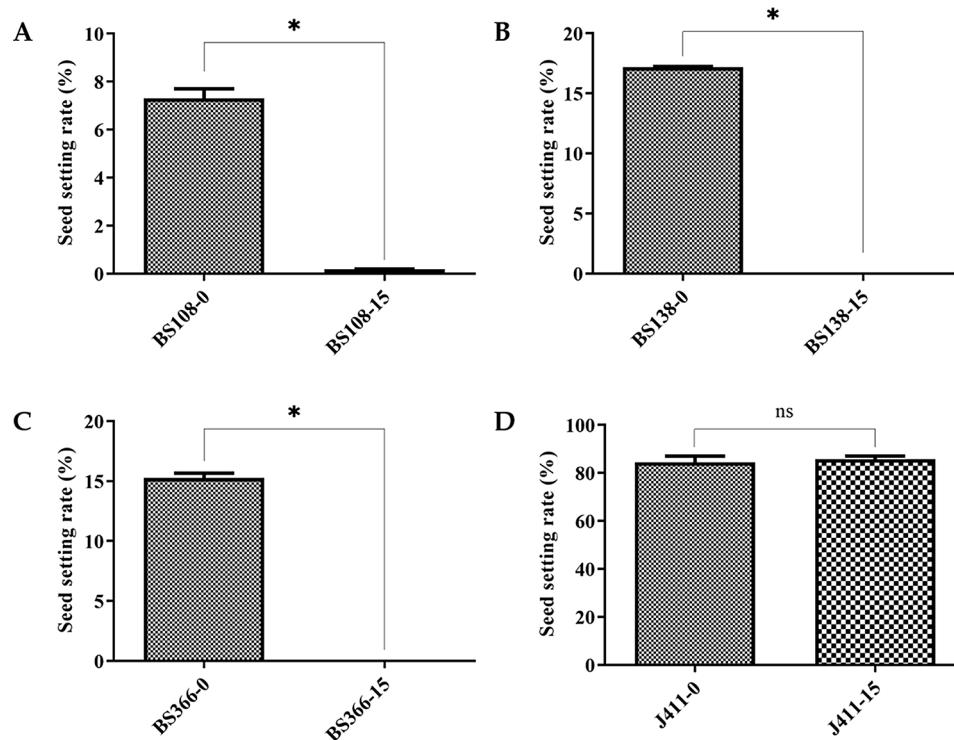


**Fig. 1** Investigation of seed setting rate under different temperature differences. **A** The seed setting rate of BS108 under 0 °C (BS108-0) and 15 °C (BS108-15) temperature differences, respectively. **B** The seed setting rate of BS138 under 0 °C (BS138-0) and 15 °C temperature (BS138-15) differences, respectively. **C** The seed setting rate of BS366 under 0 °C (BS366-0) and 15 °C (BS366-15) temperature differences, respectively. **D** The seed setting rate of J411 under 0 °C (J411-0) and 15 °C (J411-15) temperature differences, respectively. \* $p < 0.05$ ; ns, non-significant

J411 when exposed to temperature differences of 0 °C and 15 °C (Fig. 2). These findings suggested that the temperature difference of 15 °C worsened the level of male sterility in PTMS lines.

#### Summary of transcriptome data

To identify genes that respond to temperature difference and explore the molecular mechanisms, the study involved conducting transcriptome sequencing analysis on anthers at the tetrad stage from BS108 (BS108-0 and BS108-15), BS138 (BS138-0 and BS138-15), BS366 (BS366-0 and BS366-15), and J411 (J411-0 and J411-15) under temperature differences of 0 °C and 15 °C. In this analysis, three separate biological replicates were used to ensure accuracy and reliability of the results. As a result, totals of 24 samples were analyzed using transcriptome analysis. The analysis process resulted in the generation of a substantial amount of clean data, amounting to 191.633 Gb. And the average amount of clean data was found to be 7.985 Gb for each sample in this study. Additionally, the Q20 base percentage was determined to be above 95.87%, suggesting high exactitude in base calling. Similarly, the Q30 base percentage was found to be above 90.58%, further confirming the quality of the sequencing data. The samples exhibited a well-balanced composition of guanine and cytosine bases, with GC content ranging

from 50.38 to 56.67%. The transcriptome sequencing data for the samples were aligned with the wheat reference genome, resulting in alignment rates ranging from 73.492 to 90.825% (Table 2). The alignment rates achieved in this study indicate that the sequencing data can be considered reliable and adequate for conducting further analysis.

#### Identification of DEGs

The FPKM algorithm was utilized to normalize the gene expression levels. Subsequently, the screening criteria were used to identify DEGs in BS108-0 vs. BS108-15, BS138-0 vs. BS138-15, BS366-0 vs. BS366-15, and J411-0 vs. J411-15, including  $|\log_2(\text{foldchange})|$  above 1 and  $p$ -value below 0.05. In total, 20,677 DEGs were obtained in all sample under temperature differences of 0 °C and 15 °C. The results showed that 6612, 13,678, 8842, and 3737 DEGs exhibited differential expressions between BS108-0 vs. BS108-15, BS138-0 vs. BS138-15, BS366-0 vs. BS366-15, and J411-0 vs. J411-15 libraries, respectively (Fig. 3A, B). After excluding background noise (J411-0 vs. J411-15), there were 5703 DEGs detected between BS108-0 vs. BS108-15 libraries, of which 3949 were down-regulated and 1754 were up-regulated. In the BS138-0 vs. BS138-15 libraries, a comprehensive analysis identified a total of 12,076 DEGs. Among these DEGs, 7252 were found to be down-regulated, while 4824 were

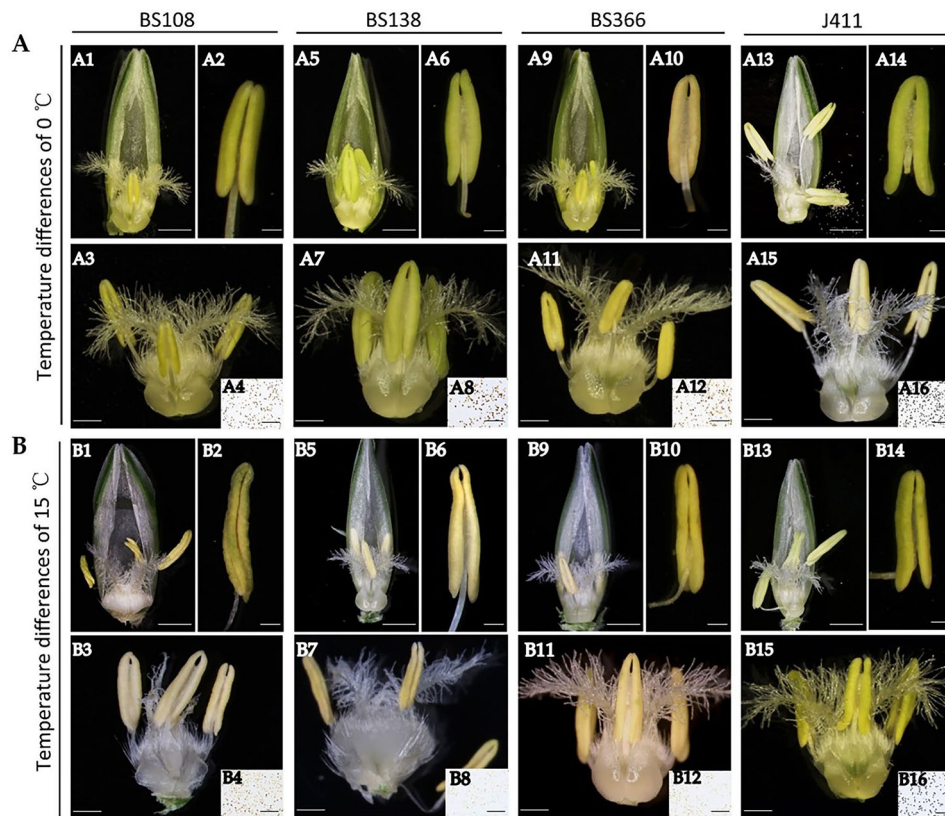


**Fig. 2** Phenotypic characteristics for PTMS lines and J411 under different temperature differences. **A** Anthers morphology and  $I_2$ -KI staining in PTMS lines and J411 under temperature differences of 0 °C. **B** Anthers morphology and  $I_2$ -KI staining in PTMS lines and J411 under temperature differences of 15 °C. Scale bars = 1 mm (A1, A5, A9, A13, B1, B5, B9, B13); 500  $\mu$ m (A3, A7, A11, A15, B3, B7, B11, B15); 300  $\mu$ m (A2, A6, A10, A14, B2, B6, B10, B14); 100  $\mu$ m (A4, A8, A12, A16, B4, B8, B12, B16)

observed to be up-regulated. Moreover, 7822 DEGs were identified in BS366-0 vs. BS366-15 libraries, with 5266 were down-regulated and 2556 were up-regulated (Fig. 3C and Table S4-S6).

In addition, 2516 genes co-expressed in BS108-0 vs. BS108-15, BS138-0 vs. BS138-15, and BS366-0 vs. BS366-15 libraries. Among the 2516 genes, BS108-0 vs. BS108-15, BS138-0 vs. BS138-15, and BS366-0 vs. BS366-15 had 300, 376, and 321 up-regulated genes, respectively, and had 2216, 2140, and 2195 down-regulated genes, respectively (Fig. S2A). The KEGG pathway analysis identified 2516 genes that were predominantly associated with “starch and sucrose metabolism”, “plant–pathogen interaction”, “galactose metabolism”, “amino sugar and nucleotide sugar metabolism”, and “phenylpropanoid biosynthesis” (Fig. S2B).

#### WGCNA of DEGs

In order to conduct a comprehensive exploration on the genes associated with DTD, we engaged in WGCNA analysis encompassing 16,940 DEGs (excluding genes from J411-0 vs. J411-15). According to the expression trend of genes, 15 modules were divided, namely

“orange”, “skyblue3”, “darkgreen”, “skyblue”, “turquoise”, “red”, “darkred”, “paleturquoise”, “darkturquoise”, “middleblue”, “greenyellow”, “lightgreen”, “darkolivegreen”, “violet”, and “grey” modules (Fig. 4A). The analysis of the relationship between modules and trait (seed setting rate) revealed a highly correlation ( $r=0.95$ ,  $p=2e-09$ ) between the “turquoise” module and DTD (Fig. 4B). In addition, the scatter plot analysis of module membership-gene significance (MM-GS) also showed a strong positive correlation between “turquoise” modules and seed setting rate among 15 modules (Fig. 5A-N). And module significance (MS) analysis showed that the MS value of “turquoise” module was the highest among all modules (Fig. 5O). The analysis of the above results revealed that the module labeled as “turquoise” played a pivotal role in understanding the effects of daily temperature fluctuations on male sterility within the study.

The analysis of GO enrichment and KEGG pathway was performed to gain a thorough understanding of the functions of the main DEGs in the “turquoise” module. The GO enrichment analysis suggested that the DEGs were significantly involved in the “polysaccharide catabolic process”, “transporter activity”, “carbohydrate

**Table 2** Statistics and evaluation of RNA-Seq data

Sample	Raw reads	Clean reads	Q20 (%)	Q30 (%)	GC content (%)	Mapped Reads (%)
BS366-0-1	74,000,070	48,698,300	96.43	91.34	53.9	86.171
BS366-0-2	66,359,160	41,482,378	96.29	91.22	54.3	80.32
BS366-0-3	69,016,558	44,182,448	96.55	91.63	53.56	85.921
BS366-15-1	70,004,498	42,433,652	96.44	91.55	53.73	82.027
BS366-15-2	81,163,904	59,039,408	96.34	91.1	51.35	73.492
BS366-15-3	72,850,340	37,730,364	95.87	90.58	54.01	82.992
BS108-0-1	81,466,158	76,311,984	97.63	93.73	52.46	89.304
BS108-0-2	78,559,800	77,204,166	97.53	93.57	52.06	90.825
BS108-0-3	84,373,382	84,226,392	96.73	91.36	50.63	90.155
BS108-15-1	84,249,120	84,090,686	97.21	92.34	50.47	90.069
BS108-15-2	92,385,182	92,269,350	96.81	91.55	50.38	89.491
BS108-15-3	102,077,808	101,872,340	97.13	92.22	50.72	89.788
BS138-0-1	70,025,590	55,030,858	96.97	92.6	53.15	82.925
BS138-0-2	67,534,082	49,270,996	96.85	92.4	52.49	75.999
BS138-0-3	77,152,876	68,047,448	97.09	92.71	52.91	83.474
BS138-15-1	78,361,288	56,362,852	96.52	91.78	53.94	76.857
BS138-15-2	66,823,216	60,617,494	97.61	93.65	51.62	86.261
BS138-15-3	76,967,294	74,921,296	97.56	93.56	51.88	85.458
J411-0-1	75,685,098	34,536,990	95.91	90.67	56.67	81.943
J411-0-2	75,199,638	41,807,406	96.51	91.47	54.23	86.488
J411-0-3	65,317,002	48,895,958	96.69	91.75	54.47	86.361
J411-15-1	69,878,202	45,539,990	96.59	91.63	54.12	85.917
J411-15-2	70,437,696	41,204,744	96.54	91.55	54.33	84.661
J411-15-3	73,077,004	48,765,810	96.61	91.5	54.36	85.712

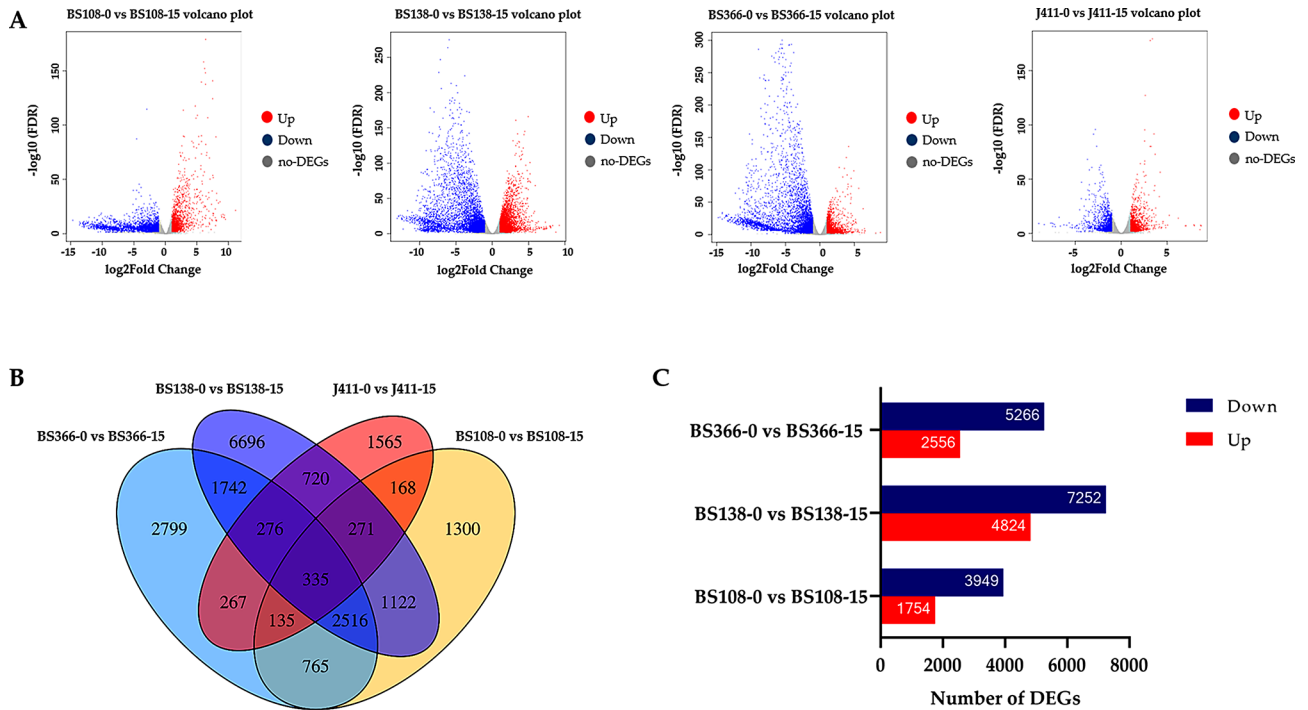


**Fig. 3** Identification of DEGs in PTMS lines and J411 under different temperature differences. **A** Volcano plots of PTMS lines and J411 under different temperature differences. **B** Venn diagram of DEGs in PTMS lines and J411. **C** Analysis of DEGs after removing background noise (J411-0 vs. J411-15)



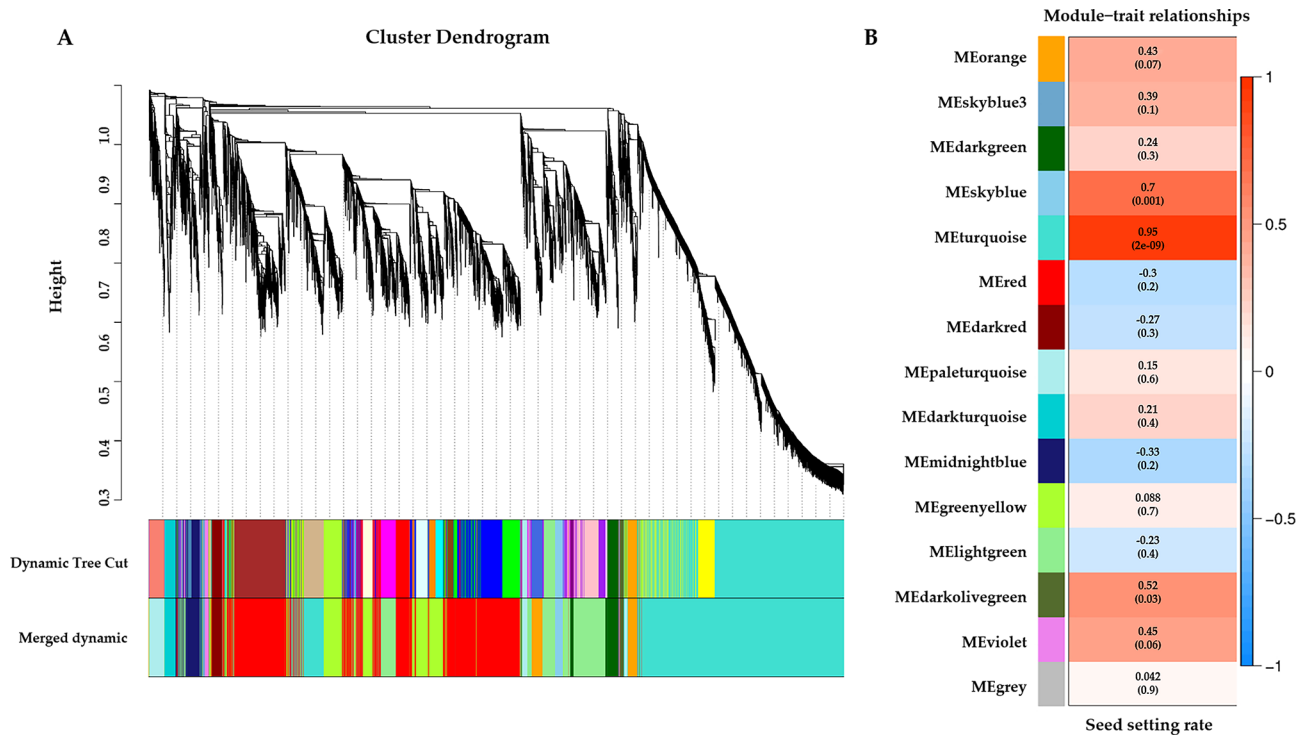


**Fig. 4** Weighted gene co-expression network analysis of DEGs. **A** Construction of cluster tree and division of module. **B** Analysis of the module– trait relationships. The left and right panels display module eigengenes and color scale, respectively

metabolic process”, “starch metabolic process”, “pollen germination”, and “pollen tube growth” (Fig. 6A). Based on the KEGG pathway analysis, it was suggested that genes associated with the “turquoise” module were linked to the metabolic processes, including “starch and sucrose metabolism”, “phenylpropanoid biosynthesis”, “MAPK signaling pathway-plant”, “flavonoid biosynthesis”, and “cutin, and suberine and wax biosynthesis” (Fig. 6B). The above biological pathways may be concerned with the temperature difference response process.

#### Expression analysis of hub DEGs

In order to comprehend the gene expression within the “turquoise” module at 0 °C and 15 °C temperature differences, all DEGs of the “turquoise” module were performed by heat map analysis. The results showed that almost all DEGs were down-regulated at a temperature difference of 15 °C, and up-regulated at a temperature difference of 0 °C (Fig. 7). In addition, we had also focused on key genes in the KEGG pathway, including the genes encoding sucrose-phosphate phosphatase (*TraesCS5D03G0004700*) and 4- $\alpha$ -glucanotransferase (*TraesCS2A03G0256000*) in “starch and sucrose metabolism”, peroxidase (*TraesCS4A03G0069100*, *TraesCS4B03G0714600*) in “phenylpropanoid biosynthesis”, mitogen-activated protein kinase (*TraesCS1D03G0975200*) and calcium-binding protein (*TraesCS4A03G0266500*) in “MAPK

signaling pathway-plant”, flavanone 3-hydroxylase (*TraesCS2A03G1151700*, *TraesCS2D03G1100600*) in “flavonoid biosynthesis”, peroxygenase (*TraesCS6D03G0660200*) and fatty acyl-CoA reductase (*TraesCS7A03G0942400*) in “cutin, and suberine and wax biosynthesis”. The heat map showed that a temperature difference of 15 °C led to the down-regulation of the key genes in the PTMS lines (Fig. 8). It can be inferred that the decrease in gene expression could potentially contribute to the aggravation of male sterility in PTMS lines when subjected to an increasing temperature difference.

#### qRT-PCR validation of hub DEGs

In order to assess the expression levels of hub genes and validate the accuracy of transcriptome data, we conducted qRT-PCR analysis. The results showed the expression levels of ten core genes associated with five important KEGG pathways significantly decreased when the temperature difference was 15 °C compared to a temperature difference of 0 °C (Fig. 9). These findings were consistent with the trends observed in the transcriptome data, further supporting the high accuracy and reliability of the transcriptome data.

#### Discussion

Wheat PTMS lines exhibited a sterile phenotype when exposed to low temperatures and short day conditions, while displayed fertility recovery under high

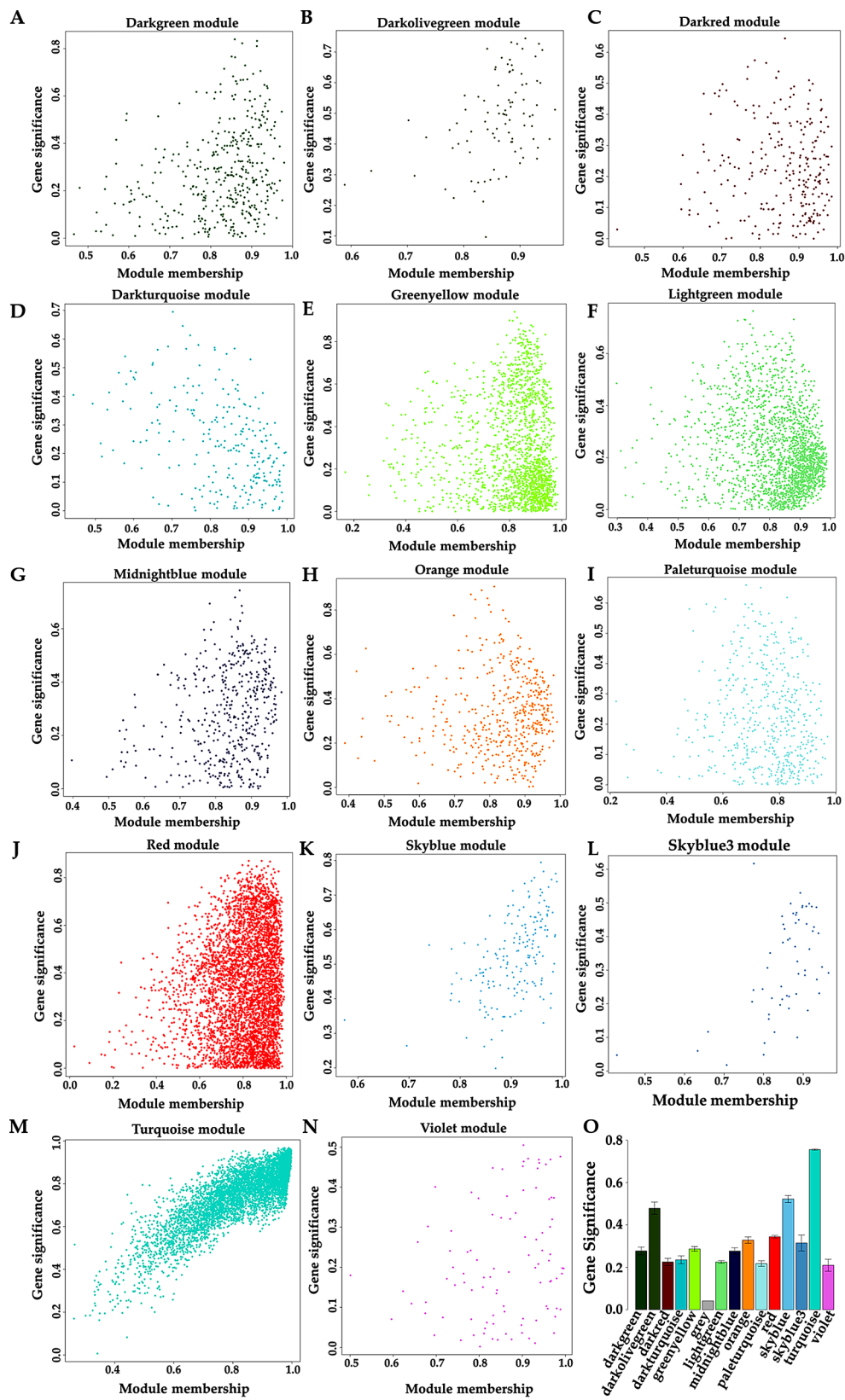


**Fig. 5** Correlation analysis between module genes and phenotypic traits. **A-N** Scatter plot analysis of module membership-gene significance (MM-GS). The horizontal axis represents the module membership (MM) of each module, and the vertical axis represents gene significance (GS). The stronger the correlation between MM and GS, the closer the relationship between this module and phenotype. **O** Analysis of module significance (MS). The MS value is obtained based on the gene significance (GS) of each gene in the module, and a larger value indicates a greater correlation with phenotypic traits

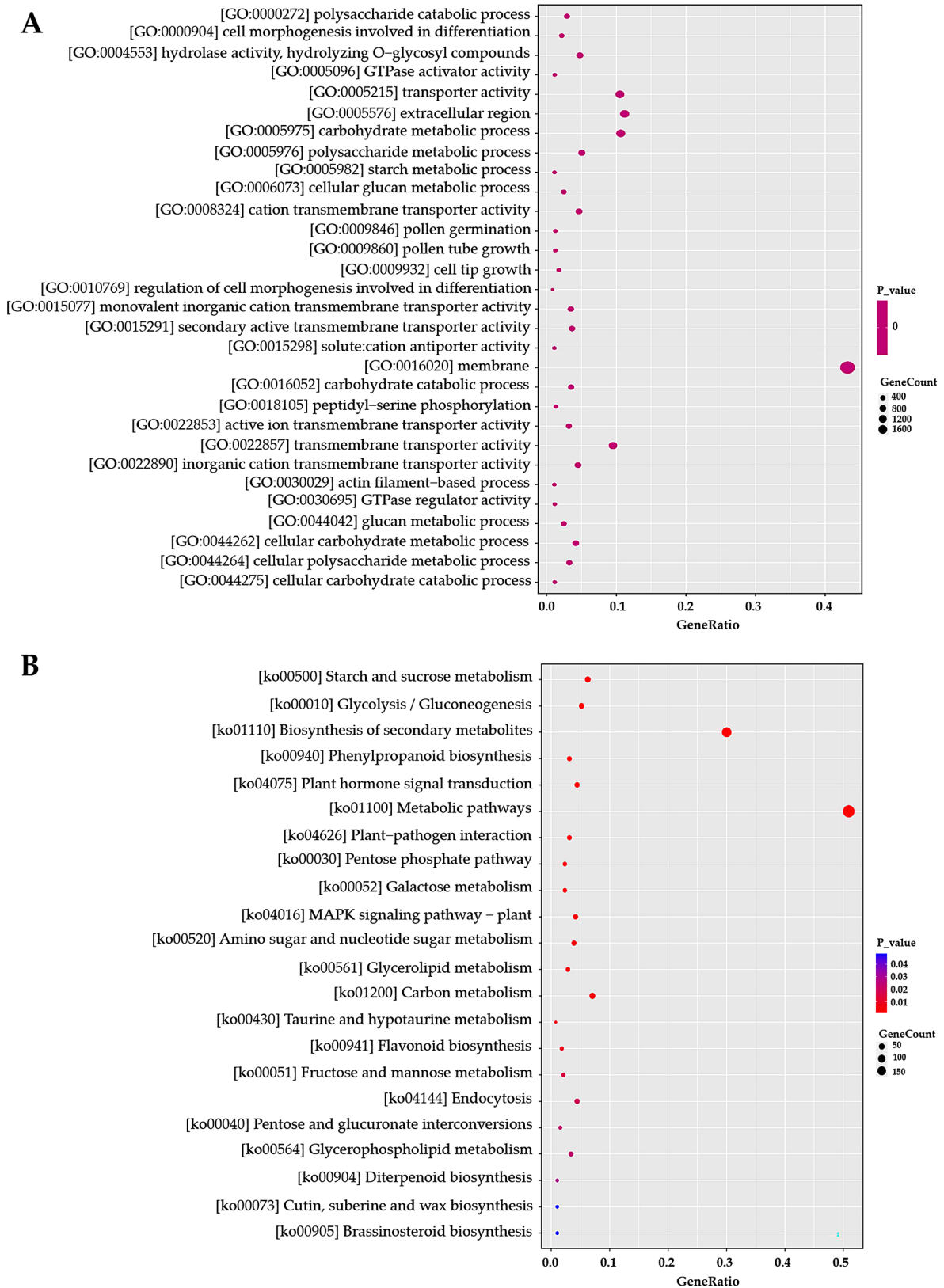


**Fig. 6** GO enrichment and KEGG pathway analysis of DEGs in the “turquoise” module. **A** GO enrichment analysis of DEGs. **B** KEGG pathway analysis of DEGs

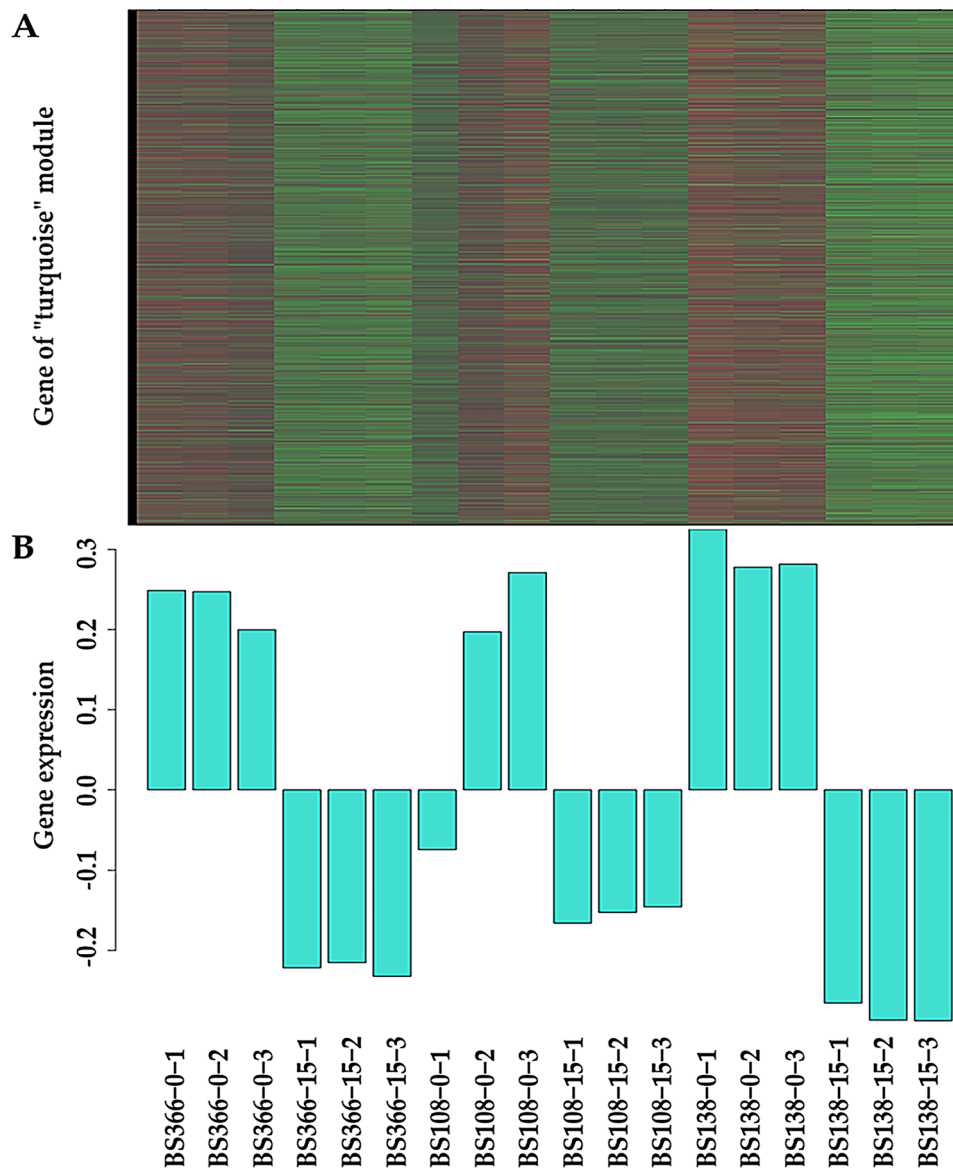


**Fig. 7** The gene expression pattern of the "turquoise" module. **A** The heat maps of genes in different samples in the "turquoise" module, with red indicating up-regulation and green indicating down-regulation. **B** The gene expression levels of different samples in the "turquoise" module. The horizontal axis represents the sample name, and the vertical axis represents the gene expression level

temperatures and long day conditions. The characteristic makes PTMS lines advantageous for ensuring secure seed production in low temperature conditions. However, the stability of fertility in PTMS lines is crucial for guaranteeing the safety of hybrid wheat seed production. Therefore, stringent measures and protocols need to be implemented to monitor and control the stability of fertility in PTMS lines. The main risks arise from self-pollination of the sterile lines and the potential purity issues resulting from fertility drift or inadequate removal of impurities during the reproductive process [3]. The issue of self-pollination necessitates stable fertility of the sterile line itself, which can be addressed by implementing technical measures such as selecting safe ecological

areas for seed production and sowing during a safe sowing period. In previous studies, safe ecological areas for seed production of PTMS lines were selected, such as Dengzhou in Henan, China and Fuyang in Anhui, China [26, 29]. In Dengzhou, five PTMS lines (BS102, BS107, BS135, BS185, and BS278) were sown from October 5th to 25th with high sterility, and all were able to produce seeds safely [25]. In this study, three PTMS lines (BS108, BS138, and BS366) were sowed under different sowing date to determine a safe sowing time in Dengzhou. The results suggested that October 5th to 25th was the best sowing time of safe seed production for three PTMS lines. Therefore, the possible optimal sowing date for the BS type PTMS lines in Dengzhou is from October 5th to



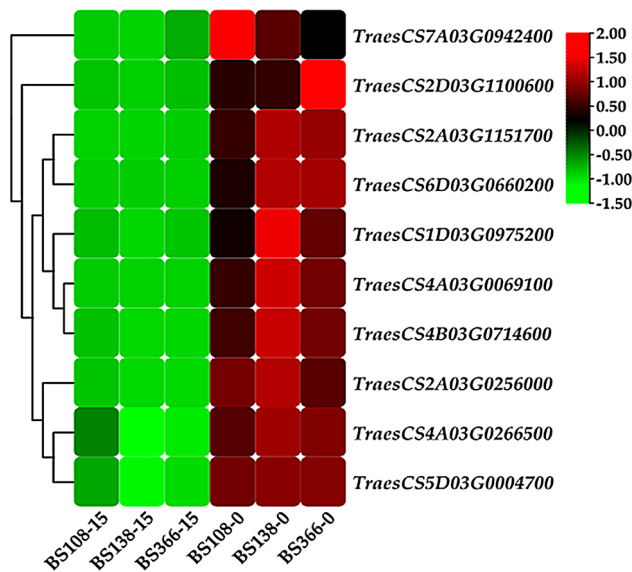


**Fig. 8** Expression analysis of key genes in important KEGG pathways

25th. The above results solidify the theoretical basis for determining the sowing date for safe seed production and the practical application of PTMS lines. And these findings offer strong support for ensuring the successful cultivation of high-quality seeds and the effective use of the PTMS lines in agricultural practices.

Ensuring the successful hybridization of wheat, particularly in relation to the PTMS lines, heavily relies on the critical aspect of safe seed production of the male sterile

lines. Proper cultivation and preservation of PTMS lines are indispensable for achieving the desired outcomes in two-line hybrid wheat development. The PTMS line serves as the foundation for the entire two-line hybrid wheat system, making it essential to prioritize the safe and effective production of seeds from the male sterile line. It is essential for ensuring the sustainability and scalability of the wheat hybridization process in order to meet the increasing demands for wheat production. Previous studies on the effect of photo-thermo conversion on fertility in wheat PTMS lines had mostly focused on average temperature, and the temperature conversion threshold obtained was also the average temperature [12, 19–22]. However, at the same average temperature, the impact of different temperature differences on fertility conversion in PTMS lines has not been reported. In the study, we conducted to examine how different temperature differences can affect the fertility of PTMS lines, while ensuring that the average daily temperature remains constant. And the objective was to reveal the safety concerns of PTMS lines seed production from the perspective of temperature difference changes. The results showed that PTMS lines exhibited more complete male sterility, with abortive pollen grains and reduced seed setting rate at a temperature difference of 15 °C compared to a temperature difference of 0 °C, indicating that increasing the temperature difference was beneficial for safe seed production of PTMS lines.

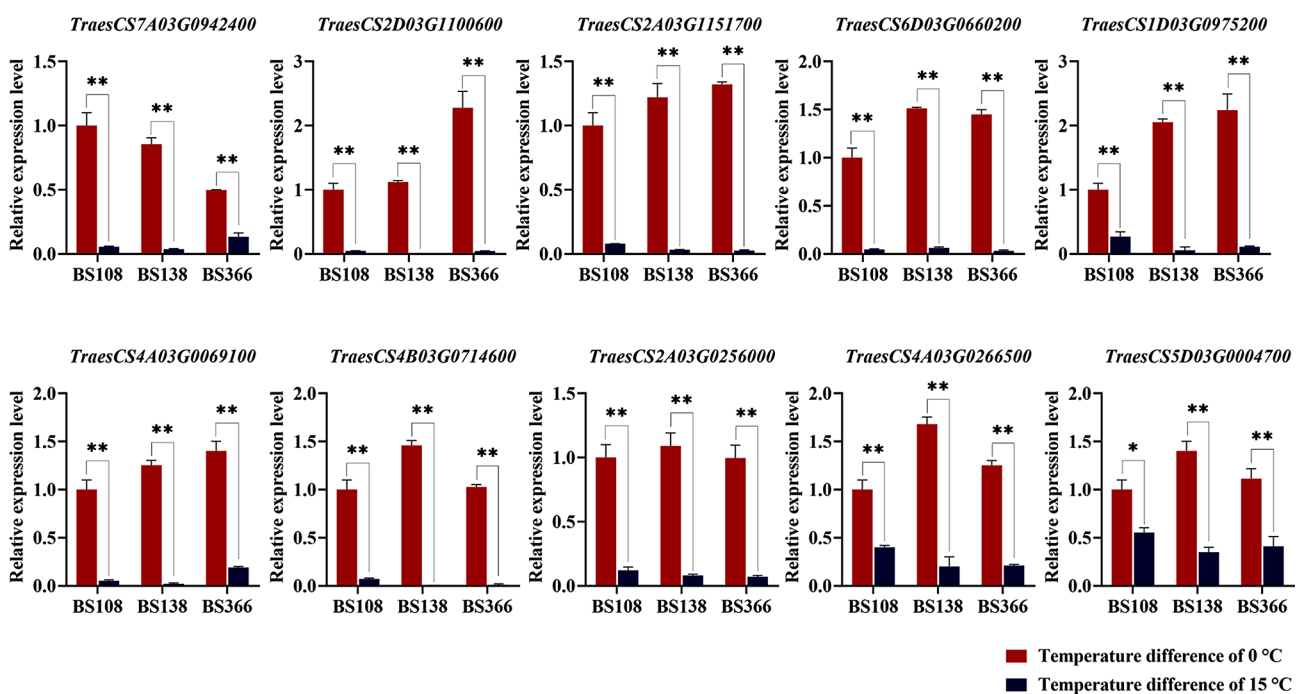


**Fig. 9** Validation of hub genes by qRT-PCR. The relative expression level was presented as  $2^{-\Delta\Delta CT}$  values and the data obtained represent three biological replicates. \*\* $p < 0.01$ , \* $p < 0.05$

Anthers, as the male organs of plants, participate in the process of pollination and reproduction, but abnormal anther development often leads to male sterility. Sucrose plays a vital role in plants' growth and progression by providing the crucial elements needed for anther and pollen development. Nevertheless, the disruption of pathways involved in "starch and sucrose metabolism" can significantly hinder pollen development, which ultimately results in male sterility [10]. Lignin, flavonoids and sporopollenin are prominent components of anther walls, and inhibition of their biosynthetic pathways may hinder the synthesis of pollen cell walls, thereby affecting fertility [26, 30]. Moreover, many investigations have shown that "MAPK signaling pathway-plant" plays an indispensable role in determining gametophyte development, embryogenesis, sporophyte formation, plant structure, and yield [31–37]. Moreover, the MAPKKK-MAPKK-MAPK module plays a crucial role in bringing together various signals from upstream and then channeling them

into different pathways downstream. It acts as a convergence point for signal transduction, where multiple pathways merge, and as a divergence point, where these merged signals split into different pathways [38]. Hence, it can be inferred that abnormal development of anthers or pollen may be caused by the obstruction of certain key pathways.

In the study, we performed a KEGG pathway analysis to examine the relationship between metabolic pathways and DEGs. The focus was on five major metabolic pathways that have significant implications in understanding molecular mechanisms and biological processes, including "MAPK signaling pathway-plant", "starch and sucrose metabolism", "phenylpropanoid biosynthesis", "flavonoid biosynthesis", and "cutin, suberine, and wax biosynthesis". By integrating the findings with previous research [10, 11, 26], we proposed a potential transcriptome-mediated network that explains the DTD affects male sterility and thus affects safe seed production of PTMS lines (Fig. 10).

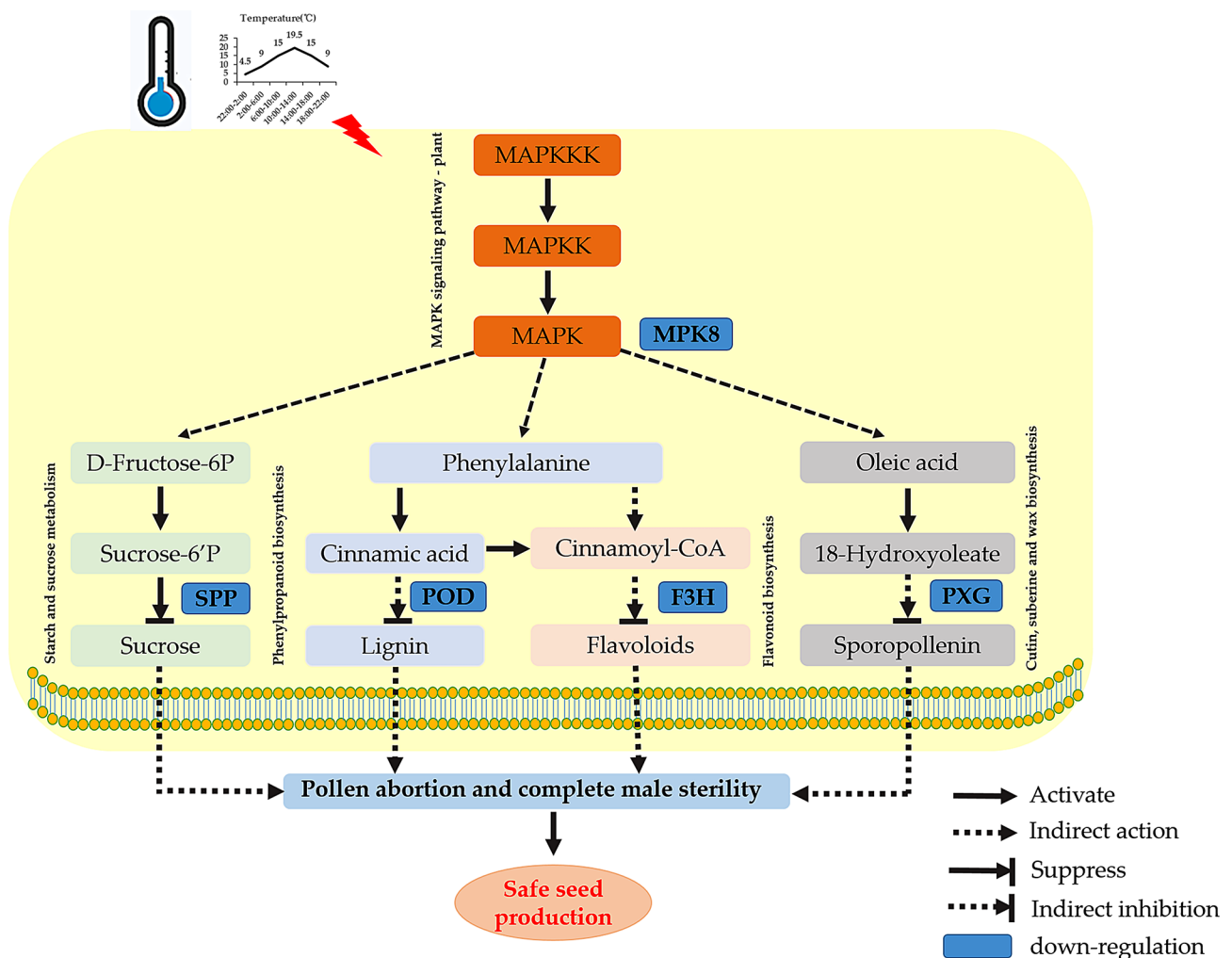


**Fig. 10** Hypothetical model of DTD affecting male sterility. MAPK, mitogen-activated protein kinase; D-Fructose-6P, D-fructose 6-(dihydrogen phosphate); Sucrose-6'P, sucrose-6-phosphate; SPP, sucrose-phosphate phosphatase; POD, peroxidase; F3H, flavanone 3-hydroxylase; PXG, peroxygenase

Under the conditions of an average temperature of 12 °C and a DTD of 15 °C, the fluctuation signal of the temperature triggers the “MAPK signaling pathway-plant”. The MAPKKK-MAPKK-MAPK module receives upstream signals and transmits them to potential downstream pathways. The decrease in MPK8 levels within the “plant MAPK signaling pathway” impacts the reduction in activity of crucial enzymes like sucrose-phosphate phosphatase (SPP), peroxidase (POD), flavanone 3-hydroxylase (F3H), and peroxygenase (PXG) in “starch and sucrose metabolism”, “phenylpropanoid biosynthesis”, “flavonoid biosynthesis”, and “cutin, suberine, and wax biosynthesis”, respectively. The down-regulation of these key enzymes inhibits the synthesis of sucrose, lignin, flavonoids, and sporopollenin, which result in abortive pollen and complete male sterility. Therefore, increasing the temperature difference exacerbates the level of male sterility, which is beneficial for the safe seed production of wheat PTMS lines.

## Conclusions

In this study, the sowing test combined with the photo-thermo-control test were used to study the sowing dates of the three PTMS lines for safe seed production, and to compare the changes in fertility of the PTMS lines under different temperature differences. The results showed that sowing seeds from October 5th to 25th and increasing the temperature difference were beneficial to the safe seed production of PTMS lines. A “turquoise” module highly correlated with temperature difference was identified using WGCNA, and the DEGs were involved in “starch and sucrose metabolism”, “phenylpropanoid biosynthesis”, “MAPK signaling pathway-plant”, “flavonoid biosynthesis”, and “cutin, and suberine and wax biosynthesis” in the module. In addition, the down-regulation of core genes in these pathways may exacerbate the degree of male sterility in PTMS lines. Our study offers a theoretical foundation and fresh perspectives on unraveling the impact of temperature difference on the secure production of PTMS line seeds.

## Abbreviations

DEGs	Differentially Expressed Genes
DTD	Daily Temperature Difference
GO	Gene Ontology
KEGG	Kyoto Encyclopedia of Genes and Genomes
PTMS	Photo-Thermo-sensitive Male Sterility
WGCNA	Weighted Gene Co-expression Network Analysis

## Supplementary Information

The online version contains supplementary material available at <https://doi.org/10.1186/s12864-024-10627-1>.

Supplementary Material 1  
Supplementary Material 2  
Supplementary Material 3

Supplementary Material 4

Supplementary Material 5

Supplementary Material 6

Supplementary Material 7

Supplementary Material 8

## Acknowledgements

The authors express our sincere gratitude to Shanghai Oringene Bio-pharm Technology Co., Ltd. for their valuable assistance in conducting high-throughput sequencing experiments.

## Author contributions

HS, LZ and XS conceived and designed the study. FN and ZL performed the experiments, analyzed the data and wrote the article with contributions from all of the authors. YL, FZ and HS provided experimental materials and participated in field trials. JB, TZ, SY, XB and CZ revised and polished this manuscript. All authors have read and agreed to the published version of the manuscript.

## Funding

This study was supported by the Beijing Municipal Natural Science Foundation (6232010); National Natural Science Foundation of China (32272108); Foundation for Youths of BAAFS (QNJJ202212); Natural Science Foundation of Beijing (6222016); Modern Agricultural Industry Technology System (CARS-03-3); The Sci-Tech Innovation 2030 Agenda (2023ZD040230309); National Natural Science Foundation of China (32072060); the Key R&D Program of Shaanxi Province (2022NY-175).

## Data availability

The original contributions presented in this study are included in this article/ in the Supplementary Materials, and the raw RNA-seq data generated in the study is available at the SRA database in National Center for Biotechnology Information (NCBI) with the accession number PRJNA1066494.

## Declarations

### Ethics approval and consent to participate

The experiments did not involve endangered or protected species. The data collection of plant materials and laboratory experiments were carried out with permission of related institution, and complied with national, and international guidelines and legislation.

### Consent for publication

Not applicable.

### Competing interests

The authors declare no competing interests.

### Author details

<sup>1</sup>College of Agronomy, Northwest A&F University, Yangling, Shaanxi 712100, China

<sup>2</sup>Beijing Key Laboratory of Molecular Genetics in Hybrid Wheat, Institute of Hybrid Wheat Beijing Academy of Agriculture and Forestry Sciences, Beijing 100097, China

Received: 4 March 2024 / Accepted: 16 July 2024

Published online: 30 July 2024

## References

1. Arya VK, Singh J, Kumar L, Kumar R, Chand P. Genetic variability and diversity analysis for yield and its components in wheat (*Triticum aestivum* L). Indian J Agr Res. 2017;51:128–34. <https://doi.org/10.18805/ijare.v0i0F.7634>.
2. Baranwal VK, Mikkilineni V, Zehr UB, Tyagi AK, Kapoor S. Heterosis: emerging ideas about hybrid vigour. J Exp Bot. 2012;63:6309–14. <https://doi.org/10.1093/jxb/ers291>.

3. Zhang AM. Strategies for hybrid wheat breeding. *Rev Chin J Agr Sci Tech*. 2002;4:42–8.
4. Geng X, Wang X, Wang J, Yang X, Zhang L, Song X. *TaEXP5* functions as a gene related to pollen development in thermo-sensitive male-sterility wheat with *Aegilops kotschyi* cytoplasm. *Plant Sci*. 2022;323:111377. <https://doi.org/10.1016/j.plantsci.2022.111377>.
5. Niu F, Bu Y, Yang X, Wu Y, He M, Xiao X, Zhang L, et al. *Rfd1*, a restorer to the *Aegilops juvenalis* cytoplasm, functions in fertility restoration of wheat cytoplasmic male sterility. *J Exp Bot*. 2023;74:1432–47. <https://doi.org/10.1093/jxb/erac484>.
6. Bu Y, Niu F, He M, Ye J, Yang X, Du Z, et al. The gene *TaPG* encoding a polygalacturonase is critical for pollen development and male fertility in thermo-sensitive cytoplasmic male-sterility wheat. *Gene*. 2022;833:146596. <https://doi.org/10.1016/j.gene.2022.146596>.
7. Guo X, Li L, Liu X, Zhang C, Yao X, Xun Z, et al. *MYB2* is important for tapetal PCD and pollen development by directly activating protease expression in *Arabidopsis*. *Int J Mol Sci*. 2022;23:3563. <https://doi.org/10.3390/ijms23073563>.
8. Yang X, Wang K, Bu Y, Ge L, Zhang L, Song X. Genome-wide analysis of *GELP* gene family in wheat and validation of *TaGELP073* involved in anther and pollen development. *Environ Exp Bot*. 2022;200:104914. <https://doi.org/10.1016/j.envexpbot.2022.104914>.
9. Song XY, Hu YG, Ma LJ, Li HB, He BR. Changes of some physiological characters in panicles of no-1B/1R and 1B/1R in K-type male sterile wheat lines. *J Triticeae Crops*. 2008;28:321–4. <https://doi.org/10.3901/JME.2008.09.177>.
10. Liu Z, Li S, Li W, Liu Q, Zhang L, Song X. Comparative transcriptome analysis indicates that a core transcriptional network mediates isonuclear alloplasmic male sterility in wheat (*Triticum aestivum* L). *BMC Plant Biol*. 2020;20:10. <https://doi.org/10.1186/s12870-019-2196-x>.
11. Zhang T, Yuan S, Liu Z, Luo L, Guo H, Li Y, et al. Comparative transcriptome analysis reveals hormone signal transduction and sucrose metabolism related genes involved in the regulation of anther dehiscence in photo-thermo-sensitive genic male sterile wheat. *Biomolecules*. 2022;12:1149. <https://doi.org/10.3390/biom12081149>.
12. Sun H, Zhang FT, Wang YB, Ye ZJ, Qin ZL, Bai XC, et al. Fertility alteration in male sterile line BS210 of wheat. *Acta Agron Sin*. 2017;43:171. <https://doi.org/10.3724/SPJ.1006.2017.00171>.
13. Tan CH, Yu GD, Yang PF, Zhang ZH, Pan Y, Zheng J. Preliminary study on the sterility of thermo-photo-sensitive genic male sterile wheat in Chongqing. *Southwest China J Agric Sci*. 1992;4:1–6. <https://doi.org/10.16213/j.cnki.scjas.1992.04.001>.
14. He JM, Dai JT, Zou YB, Zhou ML, Zhang HQ, Liu XL. Research on two line hybrid wheat I discovery, cultivation, and utilization value of ecological male sterile wheat. *Hunan Agric Sci*. 1992;5:1–3. <https://doi.org/10.16498/j.cnki.hnnykx.1992.05.001>.
15. Zhao CP, Wang X, Zhang FT, Ye ZJ, Dai HJ. Research status of hybrid wheat and thermo-photo-sensitive two line method. *Beijing Agric Sci*. 1999;17:3–5.
16. Zhao FW, Li HM, Li AG. Development, fertility transformation and fertility inheritance of a temperature sensitive male sterility of winter wheat- LT-1-3a. *J Nucl Agric*. 2001;15:65–9.
17. Zhang ZY, Hu TZ, Feng SW, Li XH, Li G, Ru ZG. A preliminary study on fertility alteration of thermo-sensitive genetic male sterile wheat line BNS. *Henan Agric Sci*. 2010;7:5. <https://doi.org/10.15933/j.cnki.1004-3268.2010.07.012>.
18. Chen XD, Sun DF, Rong DF, Peng JH, Li CD. A recessive gene controlling male sterility sensitive to short daylength/low temperature in wheat (*Triticum aestivum* L). *J Zhejiang Univ Sci B*. 2011;12:943–50.
19. Li YF, Zhao CP, Zhang FT, Sun H, Sun DF. Fertility alteration in the photo-thermo-sensitive male sterile line BS20 of wheat (*Triticum aestivum* L.). *Euphytica*. 2006;151:207–13. <https://doi.org/10.1007/s10681-006-9141-4>.
20. Zhang J, Feng L, He L, Yu G. Thermo-sensitive period and critical temperature of fertility transition of thermo-photo-sensitive genic male sterile wheat. *Chin J Appl Ecol*. 2003;14:57–60.
21. Zhou ML, Tang QY, Cheng YC, He JM. Study on the mechanism of male abortion in photoperiod-temperature sensitive genic male-sterile wheat line of ES-10. *J Hunan Agric Univ*. 1997;23:117–21.
22. Wang M, Gao Q, Yu Z, Yuan K, Yu S, Zhang B, et al. Spike differentiation process and the male sterility of BNS in wheat. *Mol Plant Breed*. 2011;9:8.
23. Guo RX, Sun DF, Cheng XD, Rong DF, Li CD. Inheritance of thermo-photoperiod sensitive male sterility in wheat. *Aust J Agr Res*. 2006;57:187–92. <https://doi.org/10.1071/AR05161>.
24. Sun H, Zhang LP, Chen ZB, Bai JF, Bai XC, Yang JF, et al. Study on photosynthetic characteristics in the BS type photo-thermal sensitive male sterile line of wheat. *J Triticeae Crops*. 2020;40:86–95. <https://doi.org/10.7606/j.issn.1009-1041.2020.01.10>.
25. Sun H, Zhao CP, Yue JR, Bai XC, Yang JF, Ye ZJ et al. Effects of different ecological environments and daily temperature difference on fertility alteration and agronomic traits in BS type photo-thermal sensitive male sterile wheat lines. *Crops*. 2023;1–8. <https://kns.cnki.net/kcms/detail/11.1808.S.20230719.1143.006.html>.
26. Liu Z, Niu F, Yuan S, Feng S, Li Y, Lu F, et al. Comparative transcriptome analysis reveals key insights into fertility conversion in the thermo-sensitive cytoplasmic male sterile wheat. *Int J Mol Sci*. 2022;23:14354. <https://doi.org/10.3390/ijms232214354>.
27. Xie C, Mao X, Huang J, Ding Y, Wu J, Dong S, et al. KOBAS 2.0: a web server for annotation and identification of enriched pathways and diseases. *Nucleic Acids Res*. 2011;39:316–22. <https://doi.org/10.1093/nar/gkr483>.
28. Chen C, Chen H, Zhang Y, Thomas HR, Frank MH, He Y, et al. TBtools: an integrative toolkit developed for interactive analyses of big biological data. *Mol Plant*. 2020;13:1194–202. <https://doi.org/10.1016/j.molp.2020.06.009>.
29. Yuan S, Bai J, Guo H, Duan W, Zhang L. QTL mapping of male sterility-related traits in a photoperiod and temperature-sensitive genic male sterile wheat line BS366. *Plant Breeding*. 2020;139:498–507. <https://doi.org/10.1111/pbr.12811>.
30. Schroter D, Baldermann S, Schreiner M, Witzel K, Maul R, Rohn S, et al. Natural diversity of hydroxycinnamic acid derivatives, flavonoid glycosides, carotenoids and chlorophylls in leaves of six different amaranth species. *Food Chem*. 2018;267:376–86. <https://doi.org/10.1016/j.foodchem.2017.11.043>.
31. Coronado MJ, González-Melendi P, Seguí JM, Ramírez C, Bárany I, Testillano PS, et al. MAPKs entry into the nucleus at specific interchromatin domains in plant differentiation and proliferation processes. *J Struct Biol*. 2002;140:200–13. [https://doi.org/10.1016/S1047-8477\(02\)00542-7](https://doi.org/10.1016/S1047-8477(02)00542-7).
32. Bush SM, Krysan PJ. Mutational evidence that the arabidopsis MAP kinase MPK6 is involved in anther, inflorescence, and embryo development. *J Exp Bot*. 2007;58:2181–91. <https://doi.org/10.1093/jxb/erm092>.
33. Guan Y, Lu J, Xu J, McClure B, Zhang S. Two mitogen-activated protein kinases, MPK3 and MPK6, are required for funicular guidance of pollen tubes in *Arabidopsis*. *Plant Physiol*. 2014;165:528–33. <https://doi.org/10.1104/pp.113.231274>.
34. López-Bucio JS, Dubrovsky JG, Raya-González J, Ugartechea-Chirino Y, López-Bucio J, de Luna-Valdez LA, et al. *Arabidopsis thaliana* mitogen-activated protein kinase 6 is involved in seed formation and modulation of primary and lateral root development. *J Exp Bot*. 2014;65:169–83. <https://doi.org/10.1093/jxb/ert368>.
35. Chao Q, Ga ZF, Wang YF, Li Z, Huang XH, Wang YC, et al. The proteome and phosphoproteome of maize pollen uncovers fertility candidate proteins. *Plant Mol Biol*. 2016;91:287–304. <https://doi.org/10.1007/s11103-016-0466-7>.
36. Chen L, Chen Q, Zhu Y, Hou L, Mao P. Proteomic identification of differentially expressed proteins during alfalfa (*Medicago sativa* L.) flower development. *Front Plant Sci*. 2016;7:1502. <https://doi.org/10.3389/fpls.2016.01502>.
37. Zhao F, Zheng YF, Zeng T, Sun R, Yang JY, Li Y, et al. Phosphorylation of SPO-ROCYTELESS/NOZZLE by the MPK3/6 kinase is required for anther development. *Plant Physiol*. 2017;173:2265–77. <https://doi.org/10.1104/pp.16.01765>.
38. Tian X, Li X, Zhou W, Ren Y, Wang Z, Liu Z, et al. Transcription factor OsWRKY53 positively regulates brassinosteroid signaling and plant architecture. *Plant Physiol*. 2017;175:1337–49. <https://doi.org/10.1104/pp.17.00946>.

## Publisher's Note

Springer Nature remains neutral with regard to jurisdictional claims in published maps and institutional affiliations.